Journal of Power Sources 196 (2011) 9961–9964

Contents lists available at ScienceDirect

Journal of Power Sources

journal homepage: www.elsevier.com/locate/jpowsour

Short communication

Low-temperature ceria-electrolyte solid oxide fuel cells for efficient methanol oxidation

Xie Meng, Zhongliang Zhan*, Xuejiao Liu, Hao Wu, Shaorong Wang, Tinglian Wen

CAS Key Laboratory of Materials for Energy Conversion, Shanghai Institute of Ceramics, Chinese Academy of Sciences (SICCAS), 1295 Dingxi Road, Shanghai 200050, China

ARTICLE INFO

Article history:
Received 12 July 2011
Received in revised form 2 August 2011
Accepted 3 August 2011
Available online 9 August 2011

Keywords:
Low temperature solid oxide fuel cells
Samarium doped ceria
Methanol

ABSTRACT

Low temperature anode-supported solid oxide fuel cells with thin films of samarium-doped ceria (SDC) as electrolytes, graded porous Ni-SDC anodes and composite $La_{0.6}Sr_{0.4}Co_{0.2}Fe_{0.8}O_3$ (LSCF)–SDC cathodes are fabricated and tested with both hydrogen and methanol fuels. Power densities achieved with hydrogen are between 0.56 W cm^{-2} at 500 °C and 1.09 W cm^{-2} at 600 °C, and with methanol between 0.26 W cm^{-2} at 500 °C and 0.82 W cm^{-2} at 600 °C. The difference in the cell performance can be attributed to variation in the interfacial polarization resistance due to different fuel oxidation kinetics, *e.g.*, 0.21 Ω cm^2 for methanol versus 0.10 Ω cm^2 for hydrogen at 600 °C. Further analysis suggests that the leakage current densities as high as 0.80 A cm^{-2} at 600 °C and 0.11 A cm^{-2} at 500 °C, resulting from the mixed electronic and ionic conductivity in the SDC electrolyte and thus reducing the fuel efficiency, can nonetheless help remove any carbon deposit and thereby ensure stable and coking-free operation of low temperature SOFCs in methanol fuels.

1. Introduction

The SOFC is an all solid-state energy conversion device that directly produces electricity from fuels with high efficiency and low emission [1]. Although traditionally intended for stationary power generation including combined heat and power [2,3], SOFCs have recently gained increasing interest for small-scale portable and transportation applications [4,5]. These applications prefer the use of high energy density fuels such as methanol, ethanol, propane and gasoline that are readily available with existing infrastructure for transport and distribution when compared to hydrogen as commonly used for fuel cells. Progress has been made in the direct utilization of these non-hydrogen fuels in SOFCs, where the coking issue at elevated temperatures were addressed by controllably operating such cells above critical current densities [6], internally reforming hydrocarbon fuels with [7,8] or without [9] an integration of a separate catalyst layer, or directly replacing the state-of-the-art nickel cermets with alternative anodes such as Cu-CeO_2 [10,11] and $Sr_2Mg_{1-x}Mn_xMoO_{6-\delta}$ [12].

The state-of-the-art SOFCs typically feature thin yttrium stabilized zirconia (YSZ) electrolytes supported on Ni-YSZ anodes and can deliver current densities of ~1.5 A cm^{-2} at 0.7 V and >750 °C [13,14]. Reduction in the SOFC operating temperature from the current 700–850 °C down to 450–600 °C would bring advantages of reduced materials cost, better manufacturing capability and enhanced durability [15,16]. Furthermore, low-temperature operation would make SOFCs much more amenable to portable and transportation applications due to faster start up and cool down. However, the reaction kinetics becomes increasingly sluggish with decreasing temperatures, thereby limiting power output for internal reforming low-temperature SOFCs, especially for hydrocarbon fuels. For example, the maximum power density for low-temperature SOFCs operating on methane via internal reforming was only 0.35 W cm^{-2} at 550 °C, but became negligibly small at 450 °C [17]. Methanol, the simplest oxygenated liquid hydrocarbon fuel, appears ideal for direct operation in low-temperature SOFCs due to less thermodynamic susceptibility to coking than other hydrocarbons and better kinetic activity due to lower bond dissociation enthalpies. There are a few reports on direct methanol-fueled SOFCs [18–22]. Jiang and Virkar demonstrated the viability of directly operating the state-of-the-art thin yttrium-stabilized zirconia (YSZ) electrolyte SOFCs with Ni-YSZ anodes on pure methanol, yielding power densities of 1.3 W cm^{-2} at 800 °C and 0.6 W cm^{-2} at 650 °C. Further reduction in the operating temperature for such cells resulted in low power densities, *e.g.*, <0.2 W cm^{-2} at 550 °C [20]. Substitution of samarium doped ceria, a higher oxygen ionic conductor, for YSZ as the thin electrolyte layer increased power densities at reduced temperatures, *e.g.*, 0.43 and 0.22 W cm^{-2} at 600 and 550 °C [21], respectively. Note that power densities as high as 0.5 W cm^{-2} at 580 °C were recently

* Corresponding author. Tel.: +86 21 6998 7669; fax: +86 21 6998 7669.
E-mail addresses: zzhan@mail.sic.ac.cn, zhongliangzhan@gmail.com (Z. Zhan).

0378-7753/$ – see front matter © 2011 Elsevier B.V. All rights reserved.
doi:10.1016/j.jpowsour.2011.08.002

demonstrated on fuel cells with carbonate-ceria composite electrolytes. However, volatility of carbonates poses almost formidable challenge on the durability of such cells [22]. In the present work, a low temperature thin film SOFC was fabricated with a finely-structured anode active layer that enabled high power densities when operating on pure methanol fuels over the temperature range of 450–600 °C.

2. Experimental

The low-temperature SOFCs consisted of thin $Ce_{0.85}Sm_{0.15}O_{1.925}$ (SDC) electrolytes, thick Ni-SDC anode supports and composite cathodes of $La_{0.6}Sr_{0.4}Co_{0.2}Fe_{0.8}O_3$ (LSCF) and SDC, and were fabricated as follows. Anode powders of SDC (Fuel Cell Materials, US) and NiO (Fuel Cell Materials, US) were ball-milled for 20 h with ethanol as the medium, then 10% starch was added and ball-milled for 4 h. The powders were dried at 80 °C, screened with 120-mesh sieve and pressed into pellets at diameters of 19 mm, which were then fired at 800 °C for 4 h. A NiO–SDC anode active layer and a thin SDC electrolyte layer were then colloidally coated on the NiO–SDC support. The colloidal solutions were prepared by ball milling the solid powder (SDC electrolyte or NiO–SDC anode) in ethanol containing appropriate amounts of dispersant and binder. The thickness of the deposited layer was controlled by the volume of the colloidal solution applied. After co-sintering of the anode substrate/active anode/electrolyte tri-layers at 1400 °C for 6 h, LSCF–SDC cathode layers were applied. LSCF–SDC cathode inks were prepared by mixing LSCF powder with SDC powder in a weight ratio of 70:30, and then mixing with a screen-printing vehicle in a three-roll mill. The cathode ink was printed onto the SDC electrolyte and fired at 1100 °C for 4 h. Then a pure LSCF current collecting layer was applied similarly and fired at 1100 °C for 4 h.

For fuel cell tests, the anode sides of the cells were sealed to alumina tubes using a ceramic adhesive (Aremco, Ultra-Temp 552). Current collector grids were painted on the electrodes using Ag inks. Single SOFCs were tested using a four-probe method in a tube furnace at temperatures from 450 °C to 600 °C. Ambient air was maintained on the cathode side. At the start of each test, humidified hydrogen was flowed through the anode compartment with the cell at 500 °C for ≈12 h, by which time the anode was reduced to Ni-SDC. After baseline testing in humidified hydrogen, methanol was fed to the anode chamber at a controlled injection rate of 0.1 ml min^{-1}. *I–V* curves and electrochemical impedance spectra (EIS) were obtained using an IM6 Electrochemical Workstation (ZAHNER, Germany). The frequency range for impedance measurement was 0.1 Hz to 100 kHz. The microstructure of these cells after testing was examined using the scanning electron microscopy (JSM6390LV, JEOL).

3. Results and discussion

Shown in Fig. 1 is a cross-sectional SEM image of the cell fractured after testing. The SDC electrolyte appeared fully dense and had a thickness of ≈6 μm. An independent gas permeability measurement of the as-fired cells before the cathode application yielded a leak rate of $<1.6 \times 10^{-18}$ m^2 that is sufficiently low as a gas-tight layer [23], *i.e.*, there were no pinholes in the thin electrolyte layer even though some isolated holes were observed. As engineered, graded porous anodes were observed for the low-temperature SOFCs. The anode supports were 0.6 mm thick and exhibited a bi-modal porous microstructure with large and small pores produced respectively from use of starch as fugitives and volume reduction associated with transformation of NiO to Ni metal. The estimated porosity was around 50%, sufficiently high to provide quick transport of fuels, especially those with large molecular weights like methanol. The active anode layers were ~12 μm thick

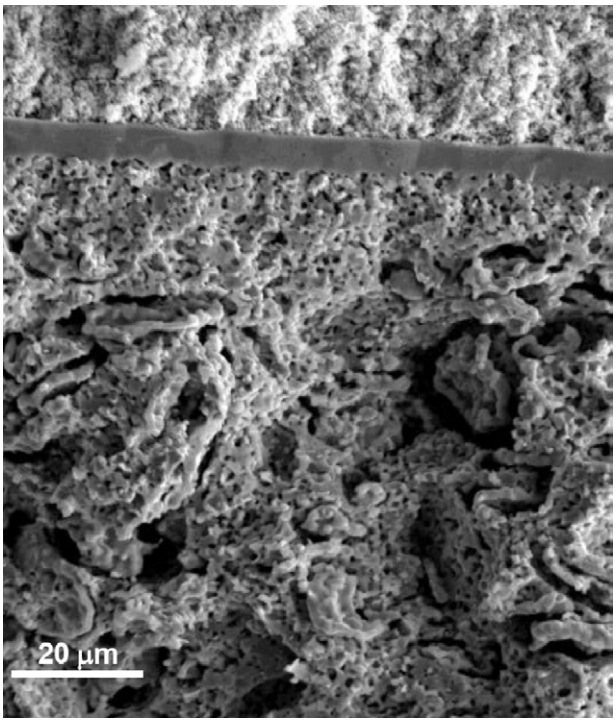

Fig. 1. Cross-sectional SEM microstructure of low temperature SOFCs.

and showed a homogeneously fine microstructure with less porosity than the anode substrates. Note that the as-fired NiO–SDC anode active layers were nearly dense since no pore former was used, such that those pores resulted primarily from NiO reduction, yielding an average pore size of 600 nm. Using the starting powder weight ratio of NiO:SDC = 60:40, the volume reduction on transformation from NiO to Ni can yield a porosity of around 29%, in good agreement with the SEM observations. Fig. 1 also shows a fine porous microstructure for the LSCF–SDC cathode and well-bonded interfaces between the electrolyte and the two electrodes.

Fig. 2a shows the voltage *V* and power density *P* versus the current density *J* for the low-temperature SOFCs directly operating on pure methanol fuel and air oxidant. The open circuit voltage (OCV) values were 0.82–0.90 V over the investigated temperature range, substantially lower than thermodynamically predicted open circuit potential (OCP) values of 1.03–1.06 V. Gas leakage through the thin electrolyte films or the surrounding ceramic seal, which would result in low OCV values, can be excluded in the present study. First, both the SEM observation and the permeability measurement indicated that the electrolyte was gas tight, as discussed above. Second, pure oxide ionic conducting YSZ-electrolyte SOFCs sealed with the same ceramic adhesive produced a nearly theoretical OCV values in hydrogen. The large difference between the measured OCV and the calculated OCP can be ascribed to the intrinsic mixed ionic and electronic conducting behaviour in SDC electrolytes that becomes less pronounced under the fuel cell operating conditions but nonetheless results in low electrical efficiencies.

The *J–V* curve at 600 °C featured a pronounced concentration polarization for $J > 2.5$ A cm^{-2}, suggesting that methanol was consumed at higher rate than available through diffusion along the 0.6 mm thick porous anode substrates. At lower temperatures, the *J–V* curves show strong activation behaviour at low current densities with no evidence of concentration polarization at high current densities. The maximum power densities measured were 0.82, 0.52, 0.26 and 0.11 W cm^{-2} at 600, 550, 500 and 450 °C, respectively. To the authors' knowledge, power

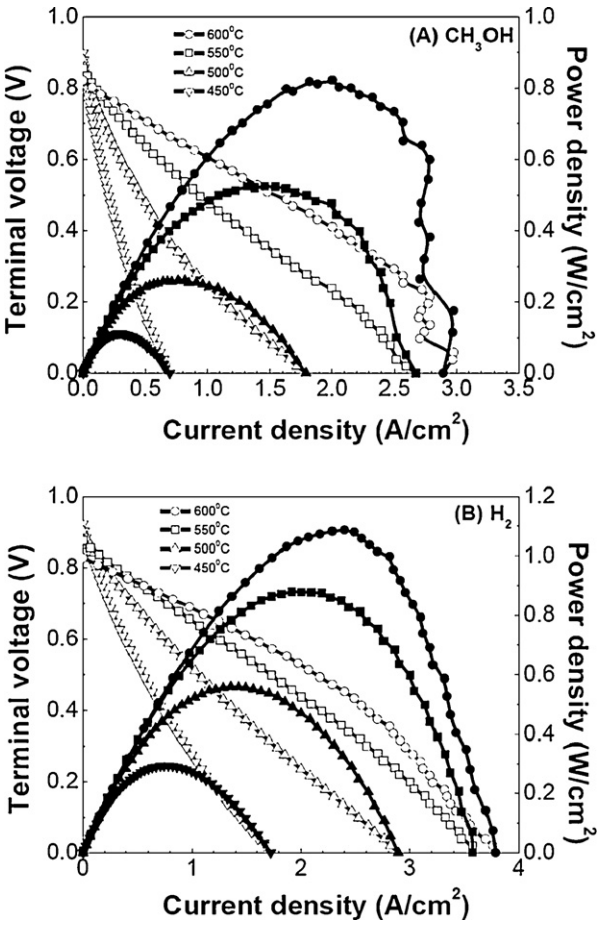

Fig. 2. Voltage and power density *vs.* current density for low temperature SOFCs operated on (a) methanol and (b) humidified hydrogen.

densities measured here are substantially higher than previously reported values for direct methanol SOFCs at similar temperatures [21,22]. Even though there is a sharp decrease in the cell performance with decreasing temperature, power densities of practical interest can be achieved at 500 °C. The present results compared favourably in terms of efficiency, durability and cost with polymer-electrolyte direct methanol fuel cells (DMFCs) [24,25] or methanol-fueled solid acid fuel cells (SAFCs) [26], where a substantial amount of water has to be mixed with methanol and noble metals like Pt and/or Ru are required.

In Fig. 2b, the polarization curves are shown for comparison of the same cell operating on humidified hydrogen. Similar OCV values were observed as in methanol fuel despite higher OCPs of 1.13–1.16 V as thermodynamically calculated. This is not surprising given that the OCV also depends on the kinetics for the electrode reactions, which are supposed to be different for the two fuels. As observed for methanol, concentration polarization also occurred at 600 °C for hydrogen even though the latter has a much higher molecular diffusion coefficient, *e.g.*, 6.1 versus 1.5 $cm^2\ s^{-1}$ for Knudsen diffusion in the present anodes with a mean pore radius of 0.3 μm. Additional enhancement in the cell performance is very likely through elaborate tailoring of the porous microstructure for both electrodes, thereby facilitating the gas transport and reducing gas-diffusion resistance. Nonetheless, maximum power densities achieved in hydrogen fuels were 1.09, 0.88, 0.56 and 0.29 $W\ cm^{-2}$ at 600, 550, 500 and 450 °C, respectively.

Electrochemical impedance spectroscopy was used to determine the ohmic and non-ohmic contributions to the cell resistance.

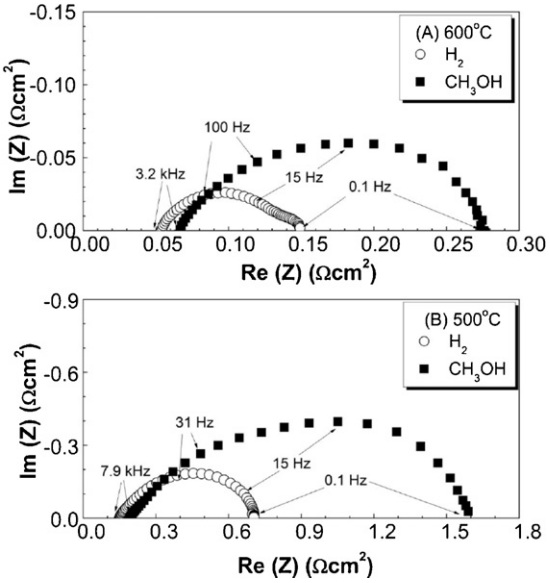

Fig. 3. Nyqusit plot of electrochemical impedance spectroscopy results from the cell at open circuits at (a) 600 °C and (b) 500 °C. Each plot compares the cells in methanol and hydrogen.

Fig. 3 shows the results of impedance spectroscopy measured at open circuits from the fuel cell operating on hydrogen and methanol at (a) 600 °C and (b) 500 °C. The high frequency intercepts correspond to the ohmic losses (R_o), whereas the difference between the high and low frequency intercepts is due to non-ohmic losses (R_p), combined polarizations from the anode and the cathode. As typical for thin-electrolyte SOFCs, the total cell resistance was dominated by the interfacial polarization, *e.g.*, 70% at 600 °C and 80% at 500 °C. The interfacial polarization resistance values were higher in methanol than in hydrogen, *e.g.*, 0.21 versus 0.10 Ω cm^2 at 600 °C. This is reasonable given that the SOFC anodes typically have more difficulty oxidizing large fuels like CO and CH_4 than oxidizing H_2 [27].

Note that the pure ohmic losses were a little bit lower in hydrogen than in methanol, *e.g.*, 0.054 versus 0.067 Ω cm^2 at 600 °C. This was probably related to temperature drop in the methanol fuel. First, decomposition of methanol over the Ni-SDC surface is endothermic, thereby decreasing the temperature of the anode and the electrolyte as well. Second, the internal heating of the SDC electrolyte is smaller due to a decrease in the leakage current. Based upon the deviation of measured OCVs from thermodynamic predicted OCPs as well as the total ohmic resistance values shown in Fig. 3a, the leakage current densities can be roughly calculated, *e.g.*, 0.80 A cm^{-2} for methanol versus 2.0 A cm^{-2} for hydrogen at 600 °C. As shown in Fig. 3b, the difference in the pure ohmic loss for the two fuels became smaller at lower temperatures due to slower decomposition of methanol and smaller leakage current density.

Prior studies have shown that the cathode material and microstructure is crucial for thin ceria-electrolyte SOFCs to achieve high power densities at low temperatures. For example, Shao and Haile [28] demonstrated that the maximum power density in hydrogen at 600 °C could attain 1.01 W cm^{-2} for a cell with a novel cathode material of $Ba_{0.5}Sr_{0.5}Co_{0.8}Fe_{0.2}O_{3-\delta}$ that exhibited superior oxygen vacancy diffusion rate than most comparable mixed conducting perovskites, but dropped substantially to only 0.50 W cm^{-2} for a similar cell with a $Sm_{0.5}Sr_{0.5}CoO_3$–SDC cathode. Ding and Hashida [15] reported that tailoring the cathode microstructure down to nano-scale can significantly increase power densities due to dramatically enlarged surface area for

oxygen reduction reactions, *e.g.*, ≈1.0 W cm^{-2} for nanostructured LSCF versus ≈0.6 W cm^{-2} for non-nanostructured LSCF. Note that a common LSCF–SDC cathode was used in the present study with non-nanostructure as fired at 1100 °C. The impressive high power densities as achieved for hydrogen as well as for methanol here can thereby ascribed to the very thin electrolytes and/or the finely structured Ni-SDC active anode layer with homogeneous pores of typically around 600 nm, providing more active sites for fuel oxidation reactions.

The mixed conductivity of the SDC electrolyte can reduce the fuel efficiency due to the leaking current. Nonetheless, efficiency is less critical for portable and transportation applications than for stationary power generators. This problem can also be partly alleviated by increasing ionic conducting domain of doped-ceria electrolytes with decreasing temperature. The ionic transference number can be roughly calculated as $t_i = V_{OC}/V_N$, where V_{oc} is the measured OCV and V_N is the thermodynamically predicted OCP that were calculated based upon the equilibrium oxygen pressure in methanol fuels relative to ambient air [29]. With temperature decreasing from 600 °C to 500 °C, the ionic transfer number increased from 0.80 to 0.85. Furthermore, under high current densities, the oxygen ions transferred from the cathode could fill the vacancies and thus deplete electrons in the electrolyte, resulting in an expansion of the pure ionic region that starts from the cathode and extends toward the anode [30]. Overall, reduction in the fuel efficiency can be minimized by decreasing the operating temperature and increasing the operating current density while maintaining reasonably power output. Note that the thin SDC electrolyte remained stable irrespective of variation of oxygen partial pressure and the ionic transference number with the current loading in the fuel cell operation [29].

Susceptibility of the anode to coking formation at elevated temperatures might be an obstacle for implementation of direct methanol-fueled SOFCs. To further evaluate the durability of such fuel cells in methanol, a few tests were conducted over a duration of 60 h, exhibiting reasonable stable power densities of 0.5 W cm^{-2} at 0.8 A cm^{-2} and 600 °C. Even though a little bit carbon deposits were detected in the anode chamber, EDX analysis of the Ni-SDC active anode layer showed no sign of coking formation. In a more extensive study, Liu et al. [21] also demonstrated impressively high stability of a similar methanol-fueled SOFC over the temperature range of 550–650 °C. Despite that coking is thermodynamically favourable for dry methanol over the temperature range of 450–600 °C, whether or not carbon deposits actually form depends on space velocity and local conditions created by coupled catalytic reforming reactions and electrochemical oxidation processes [5,31,32]. Note that methane is more susceptible to coking than methanol, but can still work stably with the Ni-YSZ anode by controlling the working current density above a critical value, which decreased with reducing the operating temperatures as a result of a decreasing coking formation rate. In particular, operating on methane fuels above a critical current density as low as 0.1 A cm^{-2} could yield stable power output at 650 °C. As a matter of fact, the leakage current density in the present ceria-electrolyte SOFCs can be as high as 0.80 A cm^{-2} at 600 °C and 0.11 A cm^{-2} at 500 °C. Carbon deposit, if any, can even be removed by oxygen introduced into the fuels via leakage current at open circuits, not to mention more oxygen available under current loadings.

4. Conclusions

In summary, we have demonstrated efficient methanol oxidation in low temperature ceria-electrolyte solid oxide fuel cells. Enhanced catalysis of finely structured anodes enables maximum power densities as high as 0.82 W cm^{-2} at 600 °C and 0.52 W cm^{-2} at 550 °C. These values are considerably larger than achieved by DMFCs or SAFCs. While extended long-term stability has yet to be demonstrated, combined features of high power densities, high fuel efficiencies, excellent CO tolerances and low costs with non noble metal catalysts would make low temperature direct methanol-fueled SOFCs highly competitive for transportation applications.

Acknowledgements

The authors gratefully acknowledge the financial support of the National Science Foundation of China under Contract No. 51072219, Science and Technology Commission of Shanghai Municipality under Contract No. 09JC1415200 and the 100 Talents Program of Chinese Academy of Sciences.

References

[1] N.Q. Minh, J. Am. Ceram. Soc. 76 (1993) 563–588.
[2] S.C. Singhal, Solid State Ionics 152 (2002) 405–410.
[3] A. Hawkes, I. Staffell, D. Brett, N. Brandon, Energy Environ. Sci. 2 (2009) 729–744.
[4] Z.P. Shao, S.M. Haile, J. Ahn, P.D. Ronney, Z.L. Zhan, S.A. Barnett, Nature 435 (2005) 795–798.
[5] M. Cimenti, J.M. Hill, Energies 2 (2009) 377–410.
[6] Y.B. Lin, Z.L. Zhan, J. Liu, S.A. Barnett, Solid State Ionics 176 (2005) 1827–1835.
[7] Z.L. Zhan, S.A. Barnett, Science 308 (2005) 844–847.
[8] Z.L. Zhan, S.A. Barnett, Solid State Ionics 176 (2005) 871–879.
[9] Z.L. Zhan, J. Liu, S.A. Barnett, Appl. Catal. A: Gen. 262 (2004) 255–259.
[10] S.D. Park, J.M. Vohs, R.J. Gorte, Nature 404 (2000) 265–267.
[11] Z.L. Zhan, S.I. Lee, J. Power Sources 195 (2010) 3494–3497.
[12] Y.H. Huang, R.I. Dass, Z.L. Xing, J.B. Goodenough, Science 312 (2006) 254–257.
[13] S.P. Simner, J.F. Bonnett, N.L. Canfield, K.D. Meinhardt, V.L. Sprenkle, J.W. Stevenson, Electrochem. Solid State 5 (2002) A173–A175.
[14] M.F. Han, Z. Liu, Z.W. Zheng, M.L. Liu, J. Power Sources 195 (2010) 7230–7233.
[15] C.S. Ding, T. Hashida, Energy Environ. Sci. 3 (2010) 1729–1731.
[16] M.F. Han, Z. Liu, L.Z. Cheng, J. Power Sources 196 (2011) 868–871.
[17] T. Suzuki, T. Yamaguchi, K. Hamamoto, Y. Fujishiro, M. Awano, N. Sammes, Energy Environ. Sci. 4 (2011) 940–943.
[18] D.J.L. Brett, A. Atkinson, D. Cumming, E. Ramirez-Cabrera, R. Rudkin, N.P. Brandon, Chem. Eng. Sci. 60 (2005) 5649–5662.
[19] M. Cimenti, V. Alzate-Restrepo, J.M. Hill, J. Power Sources 195 (2010) 4002–4012.
[20] Y. Jiang, A.V. Virkar, J. Electrochem. Soc. 148 (2001) A706–A709.
[21] M.F. Liu, R.R. Peng, D.H. Dong, J.F. Gao, X.Q. Liu, G.Y. Meng, J. Power Sources 185 (2008) 188–192.
[22] M.D. Mat, X.R. Liu, Z.G. Zhu, B. Zhu, Int. J. Hydrogen Energy 32 (2007) 796–801.
[23] P. Von Dollen, S. Barnett, J. Am. Ceram. Soc. 88 (2005) 3361–3368.
[24] X.M. Ren, M.S. Wilson, S. Gottesfeld, J. Electrochem. Soc. 143 (1996) L12–L15.
[25] R. Dillon, S. Srinivasan, A.S. Arico, V. Antonucci, J. Power Sources 127 (2004) 112–126.
[26] T. Uda, D.A. Boysen, C.R.I. Chisholm, S.M. Haile, Electrochem. Solid State 9 (2006) A261–A264.
[27] K. Eguchi, H. Kojo, T. Takeguchi, R. Kikuchi, K. Sasaki, Solid State Ionics 152 (2002) 411–416.
[28] Z.P. Shao, S.M. Haile, Nature 431 (2004) 170–173.
[29] T. Matsui, T. Kosaka, M. Inaba, A. Mineshige, Z. Ogumi, Solid State Ionics 176 (2005) 663–668.
[30] R. Doshi, V.L. Richards, J.D. Carter, X.P. Wang, M. Krumpelt, J. Electrochem. Soc. 146 (1999) 1273–1278.
[31] S. Assabumrungrat, N. Laosiripojana, V. Pavarajarn, W. Sangtongkitcharoen, A. Tangjitmatee, P. Praserthdam, J. Power Sources 139 (2005) 55–60.
[32] M. Cimenti, J.M. Hill, J. Power Sources 195 (2010) 3996–4001.